Biochimica et Biophysica Acta xxx (2014) xxx–xxx

Contents lists available at ScienceDirect

Biochimica et Biophysica Acta

journal homepage: www.elsevier.com/locate/bbapap

Antiglioma activity of GoPI-sugar, a novel gold(I)–phosphole inhibitor: Chemical synthesis, mechanistic studies, and effectiveness *in vivo* ☆

E. Jortzik [a,1], M. Farhadi [b,1], R. Ahmadi [b], K. Tóth [c], J. Lohr [b], B.M. Helmke [d,e], S. Kehr [a], A. Unterberg [b], I. Ott [f,g], R. Gust [f,h], V. Deborde [i], E. Davioud-Charvet [j,k], R. Réau [i,*], K. Becker [a,*], C. Herold-Mende [b,*]

[a] *Biochemistry and Molecular Biology, Justus Liebig University Giessen, Germany*
[b] *Division of Experimental Neurosurgery, Department of Neurosurgery, University of Heidelberg, Germany*
[c] *Division Biophysics of Macromolecules, German Cancer Research Center Heidelberg, Germany*
[d] *Institute of Pathology, Elbe Klinikum Stade, Germany*
[e] *Department of General Pathology, University of Heidelberg, Germany*
[f] *Institute of Pharmacy, Freie Universität Berlin, Germany*
[g] *Institute of Medicinal and Pharmaceutical Chemistry, Technische Universität Braunschweig, Germany*
[h] *Department of Pharmaceutical Chemistry, Institute of Pharmacy, University of Innsbruck, Austria*
[i] *UMR 6509 Institut de Chimie, CNRS Université de Rennes, France*
[j] *UMR7509 CNRS and University of Strasbourg, European School of Chemistry, Polymers and Materials (ECPM), France*
[k] *Center of Biochemistry, University of Heidelberg, Germany*

ARTICLE INFO

Article history:
Received 30 September 2013
Received in revised form 6 December 2013
Accepted 8 January 2014
Available online xxxx

Keywords:
Gold(I)–phosphole complex
Glioblastoma
Redox system
Thioredoxin reductase
Glutathione reductase
Cancer

ABSTRACT

Glioblastoma, an aggressive brain tumor, has a poor prognosis and a high risk of recurrence. An improved chemotherapeutic approach is required to complement radiation therapy. Gold(I) complexes bearing phosphole ligands are promising agents in the treatment of cancer and disturb the redox balance and proliferation of cancer cells by inhibiting disulfide reductases. Here, we report on the antitumor properties of the gold(I) complex 1-phenyl-bis(2-pyridyl)phosphole gold chloride thio-β-D-glucose tetraacetate (GoPI-sugar), which exhibits antiproliferative effects on human (NCH82, NCH89) and rat (C6) glioma cell lines. Compared to carmustine (BCNU), an established nitrosourea compound for the treatment of glioblastomas that inhibits the proliferation of these glioma cell lines with an IC_{50} of 430 μM, GoPI-sugar is more effective by two orders of magnitude. Moreover, GoPI-sugar inhibits malignant glioma growth *in vivo* in a C6 glioma rat model and significantly reduces tumor volume while being well tolerated. Both the gold(I) chloro- and thiosugar-substituted phospholes interact with DNA albeit more weakly for the latter. Furthermore, GoPI-sugar irreversibly and potently inhibits thioredoxin reductase (IC_{50} 4.3 nM) and human glutathione reductase (IC_{50} 88.5 nM). However, treatment with GoPI-sugar did not significantly alter redox parameters in the brain tissue of treated animals. This might be due to compensatory upregulation of redox-related enzymes but might also indicate that the antiproliferative effects of GoPI-sugar *in vivo* are rather based on DNA interaction and inhibition of topoisomerase I than on the disturbance of redox equilibrium. Since GoPI-sugar is highly effective against glioblastomas and well tolerated, it represents a most promising lead for drug development. This article is part of a Special Issue entitled: Thiol-Based Redox Processes.

1. Introduction

Metal-based inhibitor complexes have a high potential as anticancer agents, with platinum-based compounds such as the chemotherapeutic agent cisplatin and its derivatives being the most prominent examples. Although cisplatin acts in a highly effective manner on malignant tumor cells by forming DNA–platinum adducts, its clinical use is limited by a high systemic toxicity and fast development of cisplatin resistance in human cancer cells [1]. The success of platinum-based drugs is an arousing interest among researchers to study other metallodrugs such as ruthenium and gold complexes in the treatment of cancer [2]. Different platinum and gold-based compounds have been reported to target disulfide reductases such as thioredoxin reductase (TrxR) and/or glutathione reductase (GR), which, at least partially, mediate their

Abbreviations: AP, alkaline phosphatase; BCNU, carmustine; BUN, blood urea nitrogen; CHE, cholinesterase; Cr, creatinine; DMEM, Dulbecco's Modified Eagle Medium; GoPI, 1-phenyl-bis(2-pyridyl)phosphole gold chloride; GoPI-sugar, 1-phenyl-bis(2-pyridyl) phosphole gold chloride thio-β-D-glucose tetraacetate; GR, glutathione reductase; GSH, reduced glutathione; GSSG, oxidized glutathione; GST, glutathione S-transferase; Hb, hemoglobin; Hk, hematocrit; RBC, red blood cell count; SGOT, serum glutamate oxaloacetate transaminase; SGPT, serum glutamate pyruvate transaminase; TGR, thioredoxin glutathione reductase; TMZ, temozolomide; Trx, thioredoxin; TrxR, thioredoxin reductase; TUNEL, terminal dUTP nick end labeling; WBC, white blood cell count

☆ This article is part of a Special Issue entitled: Thiol-Based Redox Processes.

* Corresponding authors.

[1] The first two authors contributed equally to this work.

1570-9639/$ – see front matter © 2014 Elsevier B.V. All rights reserved.
http://dx.doi.org/10.1016/j.bbapap.2014.01.006

anti-tumor properties by inducing cytotoxic or antiproliferative effects [3–8]. TrxR and its substrate thioredoxin (Trx) play a major role in the homeostasis of the cellular redox state and are involved in cell proliferation by providing electrons for DNA synthesis via ribonucleotide reductase [9]. Moreover, the Trx system is closely involved in regulating apoptosis by interacting with p53, an apoptosis-regulating protein [10]. Expression levels of TrxR and Trx are often increased in aggressive tumors [11,12], and upregulation of the TrxR–Trx system has been associated with resistance to chemotherapy [13–15]. Accordingly, inhibition of the TrxR–Trx system is known to inhibit cell proliferation and to antagonize drug resistance [9,16]. GR reduces oxidized glutathione (GSSG) and thereby maintains high concentrations of reduced glutathione (GSH), which is crucial for maintaining a reducing cellular milieu. Increased levels of glutathione and upregulated GR expression have previously been observed in tumor cells [17,18]. Tumor chemoresistance has been linked to a dysregulation of the GSH system, resulting in an enhanced conjugation of different anticancer agents to GSH, which are then less toxic and exported from the cell [19]. Inhibition of GR leads to disturbances of the cellular glutathione redox potential and an increased efflux of GSSG, thereby potentially affecting the redox balance of tumor cells and decreasing resistance towards anticancer agents by reducing the formation of GSH-drug conjugates. As potential target sites for anticancer drugs, human GR has an active site with a cysteine–cysteine motif, while hTrxR has two redox-active centers with a cysteine–cysteine and a cysteine–selenocysteine pair [3,20,21]. Due to their limited aromatic character and the presence of a central nucleophilic phosphorous atom, phospholes are suitable for chemical modifications of thiols, a fact that drew our interest towards studying them as disulfide reductase inhibitors [22]. In contrast to reversible inhibitors, metal–ligand complexes are able to target the catalytic cysteine–selenocysteine pair of hTrxR and additionally interact with DNA [3]. Gold compounds exhibit a high affinity for sulfur- and selenium-containing ligands such as proteins with selenocysteine as exposed active site residues. Interestingly, gold(I)-containing complexes are at least two orders of magnitude more active on hGR than the corresponding platinum(II) or palladium(II)-containing complexes [3]. Furthermore, the gold(I) complexes are similarly active on both the seleno-hTrxR and the non-seleno-hGR. Auranofin, a phosphine-conjugated gold(I) thiosugar complex that has been developed to treat rheumatoid arthritis, inhibits TrxR from humans, bacteria, and parasites [23,24]. Auranofin and several hundred gold(I) phosphine complexes were screened as part of an antineoplastic drug development program in the '80s, which led to a large array of pharmacokinetically different series, including the chlorophosphine gold(I) complexes – from the simplest Et_3PAuCl to the lipophilic Ph_3PAuCl – the various gold(I) thiolates; and alkyl, aryl, alkoxy, and amino-substituted phosphine–gold complexes [25]. The structure–activity relationships have shown that the structural changes within ligand types coordinated to the gold atom, which govern the lipophilic character, distribution, and partition coefficients as part of the pharmacokinetics, can profoundly alter the cytotoxicity of the gold(I) complexes both *in vitro* and *in vivo*. Furthermore, as previously reported, both auranofin **4** and its gold(I) chlorotriethyl phosphine were shown to act as prodrugs *in vivo*, and function via a bioactivation process involving the transient displacement of the thiosugar moiety or the chlorine atom by (redox) protein(s) or low molecular weight thiols before irreversibly binding to the common final DNA target. Both the chlorine atom and the thiosugar part are known leaving groups displaced by cysteine and histidine residues of albumin [26–29]. Following different reversible exchanges with thiol groups or proteins in the blood, these gold(I) complexes are known to bind DNA: interaction of auranofin **4** or gold(I) chlorotriethyl phosphine led to the formation of the same gold(I)–DNA complex [30].

Interestingly, auranofin was recently reported to inhibit the worm protein thioredoxin–glutathione reductase (TGR) from *Schistosoma mansoni* parasites, which also contains a selenocysteine at the penultimate C-terminal part [31–33]. As for hGR alkylated by the gold–phosphole complex GoPI [3], the X-ray structure of wild type TGR incubated with auranofin showed an almost linear S–Au(I)–S-coordination in the active site following the release of both the leaving group and the phosphine moiety [31]. "Auranofin-like" gold(I) complexes containing thiocyanate or xanthate affect TrxR activity in a low nanomolar range and inhibit GR, but they do so less effectively with IC_{50} values in the micromolar range. Furthermore, they have antiproliferative effects on several human cancer cell lines [6].

Currently, temozolomide (TMZ) is the treatment of choice for glioblastomas, a highly malignant primary brain tumor, and has mostly replaced the currently used nitrosourea-based drugs such as carmustine because it has a low toxicity and is easy to administer [34]. However, the prognosis for patients with a glioblastoma remains poor, with a high recurrence rate and a 5-year chance of survival of 9.8% [35]. A range of structurally diverse gold(I) complexes has been studied as agents for the treatment of cancer [36,37]. Among them are gold(I) phosphine complexes [5,6], gold(I) carbene complexes [8,38], alkynyl gold(I) complexes [39], gold(I) complexes of imidazole and thiazole-based diphos type ligands [40], and azolate gold(I) phosphane complexes [7]. All of them demonstrate an anticancer activity by exhibiting antiproliferative or cytotoxic effects, and many of them were shown to target human thioredoxin reductase. We previously have shown that the complex 1-phenyl-bis(2-pyridyl)phosphole gold chloride (GoPI) is a highly potent inhibitor of human GR and TrxR, with IC_{50} values in the low nanomolar and micromolar range, respectively. Gold(I)-containing phosphole complexes competitively inhibit hGR by competing with GSSG. (Phosphine)gold chloride complexes thereby act as prodrugs with stepwise ligand displacement resulting in a covalently bound gold atom between the two active site cysteines of hGR (S–Au–S coordination) [3]. The binding mode of GoPI to hTrxR appears to be more complex due to the presence of two redox-active sites, with a selenocysteine in the C-terminal active site being mainly, but not exclusively, targeted (S–Au–Se coordination) [3,31]. It has been suggested that the selenocysteine likely mediates the transfer of gold from its phosphine ligands in GoPI or auranofin complexes to the redox-active Cys pair of TrxR or TGR. In addition to disulfide reductase inhibition, the antiproliferative effects of GoPI on glioblastoma cells can be mediated by binding to DNA [3]. However, GoPI is unstable due to a release of the chloride ligand in aqueous solutions. A sugar-linked form of GoPI, the complex 1-phenyl-bis(2-pyridyl) phosphole gold chloride thio-β-D-glucose tetraacetate (GoPI-sugar) was synthesized based on the structures of GoPI and auranofin and has improved solubility, stability, and bioavailability. GoPI-sugar inhibits the human breast cancer cell line MCF-7 with IC_{50} values of around 2 μM by triggering nuclear fragmentation and chromatin condensation, which are indicative of apoptosis, and perturbing the cell cycle. Interestingly, GoPI-sugar irreversibly inhibits hTrxR in MCF-7 cells (IC_{50} = 1.9 μM) but does not affect hGR activity [41]. Thus, GoPI-sugar shows cytotoxic and cytostatic effects on human breast cancer cells, which seem to be at least partially mediated by inhibition of hTrxR [41]. This motivated us to study the effects of GoPI-sugar on glioblastomas, the most common and lethal type of brain tumors. Glioblastomas, which typically harbor mutations of p53, usually show increased levels of TrxR, indicating that the Trx system is involved in glial neoplastic diseases [11]. As delineated below, GoPI-sugar indeed inhibits the proliferation of glioma cells in vitro and in vivo with tolerable side effects.

2. Material and methods

2.1. GoPI-sugar synthesis

Sodium hydride (37.7 mg, 1.5 mmol) was added to a solution of 1-thio-β-D-glucose tetraacetate (272 mg, 0.75 mmol) in tetrahydrofuran (25 mL). The heterogeneous mixture was stirred for 1 h at room

Please cite this article as: E. Jortzik, et al., Antiglioma activity of GoPI-sugar, a novel gold(I)–phosphole inhibitor: Chemical synthesis, mechanistic studies, and effectiveness *in vivo*, Biochim. Biophys. Acta (2014), http://dx.doi.org/10.1016/j.bbapap.2014.01.006

temperature. The solution was filtered and added to a tetrahydrofuran solution (20 mL) of 1-phenyl-2,5-bis(2-pyridyl)phosphole gold complex **1** (408 mg, 0.68 mmol) [3]. The solution was stirred for 90 min at room temperature, and all volatile materials were removed under vacuum. After purification by column chromatography on silica gel (diethyl ether/ethyl acetate: 7/3), complex **2** was obtained as a yellow powder (436 mg, yield 70%). A patent for GoPI-sugar was registered (EP1771181B1).

^{1}H NMR ($CDCl_3$, 300.1 MHz): δ = 1.81 (s, ^{3}H, CH_3), 1.85 (m, 4H, =CCH_2CH_2), 2.02 (s, 3H, CH_3), 2.03 (s, 3H, CH_3), 2.10 (s, 3H, CH_3), 3.01 (m, 2H, =CCH_2CH_2), 3.32 (m, 2H, =CCH_2CH_2), 3.69 (ddd, 1H, J_{HH} = 2.1 Hz, J_{HH} = 4.5 Hz, J_{HH} = 9.9 Hz, CH), 4.00 (dd, 1H, J_{HH} = 2.1 Hz, J_{HH} = 12.3 Hz, CH), 4.10 (dd, 1H, J_{HH} = 2.1 Hz, J_{HH} = 12.3 Hz, CH), 4.94 (t, 1H, J_{HH} = 9.9 Hz, CH), 5.04 (m, 3H, CH_2, CH), 7.09 (2dd, 2H, J_{HH} = 4.8 Hz, J_{HH} = 7.8 Hz, H_5 Py), 7.29 (m, 3H, *m*-Ph, *p*-Ph), 7.63 (2dd, 2H, J_{HH} = 7.8 Hz, J_{HH} = 7.8 Hz, H_4 Py), 7.75 (2d, 2H, J_{HH} = 7.8 Hz, H_3 Py), 7.79 (d, 2H, J_{HH} = 8.1 Hz, *o*-Ph), 8.56 (2d, 2H, J_{HH} = 4.8 Hz, H_6 Py) ^{13}C{^{1}H}NMR ($CDCl_3$, 75.5 MHz): δ = 20.6 (s, CH_3), 20.7 (s, CH_3), 20.8 (s, CH_3), 21.2 (s, CH_3), 22.4 (d, J_{PC} = 3.1 Hz = CCH_2CH_2), 29.6 (d, J_{PC} = 9.0 Hz, =CCH_2), 29.7 (d, J_{PC} = 9.1 Hz, =CCH_2), 62.8 (s, CH_2 sucre), 68.9 (s, CH sucre), 74.3 (s, CH sucre), 75.6 (s, CH sucre), 77.7 (s, CH sucre), 83.1 (s, CH sucre), 122.0 (s, C_5 Py), 122.2 (s, C_5 Py), 123.9 (d, J_{PC} = 6.5 Hz, C_3 Py), 124.1 (d, J_{PC} = 6.3 Hz, C_3 Py), 126.5 (d, J_{PC} = 56.9 Hz, *i*-Ph), 128.8 (d, J_{PC} = 12.1 Hz, *m*-Ph), 131.4 (d, J_{PC} = 2.6 Hz, *p*-Ph), 134.2 (d, J_{PC} = 14.0 Hz, *o*-Ph), 134.6 (d, J_{PC} = 58.0 Hz, =CP), 135.1 (d, J_{PC} = 58.0 Hz, =CP), 136.3 (s, C_4 Py), 149.3 (d, J_{PC} = 6.0 Hz, C_6 Py), 149.4 (d, J_{PC} = 5.6 Hz, C_6 Py), 152.3 (d, J_{PC} = 15.8 Hz, C_2 Py), 152.5 (d, J_{PC} = 16.1 Hz, C_2 Py), 152.9 (d, J_{PC} = 14.0 Hz, *C* = CP), 153.5 (d, J_{PC} = 14.0 Hz, *C* = CP), 169.5 (s, C=O), 169.6 (s, C=O), 170.2 (s, C=O), 170.8 (s, C=O). ^{31}P{^{1}H} NMR ($CDCl_3$, 121.5 MHz) δ = +46.7 ppm (s). HR-MS (ESI, CH_2Cl_2): *m/z* 951.1768 ($M^+ + Na^+$: calculated 951.1755).

2.2. DNA melting curves

Linearized PUC 18 plasmid DNA was incubated with 1–20 μM **1** in degassed 10 mM phosphate pH 7.0 containing 1% dioxan (ratio of 1 to number of basepairs **1**–**4**:20–1:1). Thermal denaturation curves were recorded between 50 and 97 °C (0.5 °C/min) at 260 nm (hyperchromic effect) on a Cary 4E spectrophotometer (Varian, Mulgrave, Australia). After normalization to absorbance at room temperature and smoothing in five-point intervals, derivative melting curves of the samples were drawn (KaleidaGraph™).

2.3. Gel motility studies

Superhelical DNA (pUC18) was incubated with topoisomerase I (Invitrogen) and varied concentrations of complexes **1**, **3**, and **4**. Incubation conditions were optimized by varying incubation time (1 to 2 h), the amount of topoisomerase I (calf thymus from Invitrogen or wheat germ from Promega), and the reaction buffer. All incubations were performed at 37 °C without shaking. After incubation, an equal volume of phenol/chloroform/isoamylalcohol was added to the sample, mixed thoroughly, and centrifuged for 5 min at 35,000 *g* at room temperature. The upper (aqueous) phase was collected, and an equal volume of phenol/chloroform/isoamylalcohol was added and centrifuged as described above. The upper phase was collected. No further chloroform and ether extractions were done, since phenol does not interfere with gel electrophoresis. 1% agarose gels were run in TBA buffer for 200 min at constant 8 V/cm and 200 mA. 0.1 μg DNA sample and a 1 kb marker from Bioron was loaded onto the gel. For visualization the gels were stained with ethidium bromide.

2.4. Cell culture conditions

The malignant rat glioma cell line C6 (ATCC, Rockville, MD) as well as NCH82 and NCH89 cells established from human glioblastoma tissues [42] were cultured in Dulbeco's Modified Eagle Medium (DMEM) supplemented with 10% fetal calf serum and antibiotics (100 units/mL penicillin and 100 μg/mL streptomycin) at 37 °C in a humidified atmosphere with 5% CO_2 and 95% air. Medium changes were performed twice a week. After reaching confluence, cells were harvested by a brief incubation with a trypsin/EDTA solution (Viralex, PAA, Linz, Austria) and seeded into a fresh 75 cm^2 plastic tissue culture flask.

2.5. Proliferation assay

Quantification of DNA synthesis was performed using the BrdU Labeling and Detection Kit III (Roche Diagnostics, Mannheim, Germany) as described [43]. Tumor cells were seeded in 8 replicates on 96-well plates. For the proliferation assay after chemotherapy, GoPI-sugar was administered in different concentrations 24 h after seeding and incubated for 72 h. Optical density was determined, and the means of control samples were defined as 100% proliferation rate. Values are means of at least two independent experiments.

2.6. Orthotopic glioma model

Male 6 to 8-week-old Wistar rats were used (Charles River, Wiga, Germany). Institutional guidelines for animal welfare and experimental conduct were followed. After an intracranial injection of 2×10^5 C6 glioma cells [44], animals were repeatedly (on days 3, 5, 7, and 9 post-implantation) treated intravenously with two different doses of GoPI-sugar (22 mg/kg body weight or 30 mg/kg body weight). Control animals received 500 μL of the vehicle intravenously (10% DMF and 10% Chremophor (1:1), adjusted to 100% with NaCl). Analysis of tumor growth and response to therapeutic interventions was performed via repetitive MRI scanning using a 2.35 T small bore MRI unit (Biospec 24/40, BRUKER Medizintechnik, Ettlingen, Germany) as described [44]. Body weight and neurological symptoms were recorded every two days. All rats were euthanized via decapitation on day 16 after tumor cell implantation, and the vital organs including contralateral brain, liver, kidney, as well as muscles were immediately snap frozen in liquid nitrogen and stored at −80 °C until processing for further histological and biochemical analyses. Prior to euthanization, whole blood samples were collected in order to assess potential treatment-induced drug toxicity by measuring hemoglobin (Hb), platelet count, white blood cell (WBC) count, red blood cell (RBC) count, creatinine (Cr), serum glutamate oxaloacetate transaminase (SGOT), serum glutamate pyruvate transaminase (SGPT), blood urea nitrogen (BUN), alkaline phosphatase (AP), and bilirubin. Furthermore, the oxidative status of the blood samples was analyzed as described below.

For this purpose the tissues of treated and untreated animals were taken, weighed, homogenized using a dounce homogenizer, and analyzed according to a previously published atomic absorption spectroscopy method [45]. Gold levels are indicated as ng gold per g tissue.

2.7. Ki-67 staining and in situ apoptosis assay

To distinguish between proliferating cells and those undergoing apoptosis, 5 μm cryostat sections were prepared from tumor xenografts. In order to assess proliferation in tumor xenografts, cryostat sections were incubated with a Ki-67 antibody (mouse monoclonal antibody, 10 μg/mL, BD Pharmingen, Hamburg, Germany) for 1 h. Detection was performed as described [42]. To measure apoptotic cells, a terminal dUTP nick-end labeling (TUNEL) assay was performed using an *in situ* apoptosis detection kit according to the manufacturer's instructions (Boehringer Mannheim, Mannheim, Germany). The Ki-67-positive and apoptotic cells were counted per visual field on 3 hotspots at ×20

Please cite this article as: E. Jortzik, et al., Antiglioma activity of GoPI-sugar, a novel gold(I)–phosphole inhibitor: Chemical synthesis, mechanistic studies, and effectiveness *in vivo*, Biochim. Biophys. Acta (2014), http://dx.doi.org/10.1016/j.bbapap.2014.01.006

magnification using the AnalySIS image analysis software (Soft Imaging System, Muenster, Germany). Counting was performed in a blinded manner. Finally, mean values were calculated.

2.8. Tissue preparation

Tissues from control and GoPI-sugar-treated rats were kept frozen in liquid nitrogen, pulverized in a mortar and solved in 100 mM potassium phosphate buffer, 2 mM EDTA, pH 7.4. After freezing and thawing three times, the homogenized tissues were lysed by sonication and centrifuged at 35,000 *g* and 4 °C for 30 min. The clear supernatant was directly used in enzyme assays.

2.9. Tissue samples, protein and enzyme assays

The protein concentration of the tissue samples was determined photometrically at 595 nm using the Bradford assay and a bovine serum albumin calibration curve. All activity assays with tissue samples were carried out at 37 °C with pre-warmed substrates. All measurements were done at least in duplicate. Data and mean values ± SD were calculated for each therapeutic group.

As the TrxR activity was supposed to be low in some of the tissues, the sensitive DTNB-reducing activity of the enzyme was determined. TrxR activity was measured in 100 mM potassium phosphate, 2 mM EDTA, pH 7.4 with 3 mM DTNB as the substrate (100 mM stock solution in DMSO). TNB^- production was monitored at 412 nm, and the activity was calculated using $\varepsilon_{TNB} = 13.6\ mM^{-1}\ cm^{-1}$. Non-NADPH-dependent reduction of DTNB was determined for each sample and subtracted. The NADPH-dependent Trx-reducing activity of hTrxR was measured by following the oxidation of NADPH spectrophotometrically at 340 nm as described elsewhere [46].

The assay for measuring the activity of GR contained 47 mM potassium phosphate, 1 mM EDTA, 200 mM KCl, pH 6.9, 100 μM NADPH, and 2 μM FAD. After adding tissue extract, the reaction was started with 1 mM GSSG. The oxidation of NADPH was monitored via a decrease in absorbance at 340 nm. Adding FAD to the assay mixture allows one to determine total GR (holoGR + apoGR) [44].

Glutathione peroxidase (GPx) assays were performed in 100 mM Tris, 1 mM EDTA, pH 8.0, 2 mM GSH, 1.0 U/mL PfGR, and 100 μM NADPH [44]. After adding tissue extract and incubating for 5–10 min, the assay was started by adding 70 μM *tert*-butylhydroperoxide. A reference cuvette containing all components without tissue extract was used as a control.

Glutathione *S*-transferase (GST) activity was determined in 100 mM HEPES, 1 mM EDTA, pH 6.5 with 1 mM GSH and 500 μM CDNB [44]. A reference cuvette containing all components without a tissue sample was used as a control.

2.10. Blood samples, protein and enzyme assays

To lyse erythrocytes in whole blood samples, digitonin was added at a final concentration of 40 μg/mL to the different assay buffers. The hemoglobin concentration in the whole blood samples was estimated as follows: concentration (Hb) = (A_{340nm} of sample Hb − A_{340nm} of lysis assay buffer) × D / 18.5; with D = dilution factor for the blood sample, factor 18.5 = $\varepsilon_{340\ nm}\ (g/dL)^{-1}\ cm^{-1}$ [44]. The activities of GR, GPx, and GST in whole blood samples had already been determined in Section 2.9 for the tissue samples.

2.11. Measurement of glutathione concentrations

Total glutathione concentrations in whole blood as well as in different tissue samples were measured as described previously [44]. Briefly, one volume of fresh EDTA blood was mixed with two volumes of 5% sulfosalicylic acid (w/v). After centrifugation for 10 min at 10,000 *g*, 10 μL of supernatant was transferred in a total volume of 500 μL 143 mM sodium phosphate, 6 mM EDTA, pH 7.5, 0.6 mM DTNB, 0.5 U/mL GR, and 0.3 mM NADPH. The increase in absorbance due to reduction of DTNB was monitored at 412 nm and 25 °C. The glutathione concentration was calculated using a standard curve. The concentration of glutathione in erythrocytes was estimated on the basis of whole blood glutathione and the hematocrit ($[GSH]_{Ery} = [GSH]_{blood} \cdot 100 / Hk_{\%}$) [44].

2.12. Inhibition studies

For the inhibition studies, hGR and hTrxR were produced as described previously (recombinant hGR [47] with a specific activity of 60–120 U/mg, wild type hTrxR isolated from human placenta [48] with 16 U/mg activity as determined in the DTNB assay, and recombinant $hTrxR^{U498C}$ [49] with 0.46 U/mg as determined in the DTNB assay). In order to test the inhibition of recombinant enzymes, both compounds GoPI and GoPI-sugar were dissolved in DMF. hGR inactivation was measured in the GSSG reduction assay as described above in Section 2.9. For hTrxR, inactivation of the wild type and the selenocysteine-lacking mutant $hTrxR^{Sec498Cys}$ was measured with the DTNB and Trx reduction assays (see Section 2.9.). The following final concentrations of redox enzymes were employed in the assays for IC_{50} determinations: 1.4–2.8 nM hGR, 3.7 nM wild type hTrxR (DTNB assay), 30 nM wild type hTrxR (thioredoxin reduction assay), 140–280 nM $hTrxR^{U498C}$ (DTNB assay), and 3 μM $hTrxR^{U498C}$ (thioredoxin reduction assay). Half-maximal inhibition of the enzymes (IC_{50}, analyzed with GraphPad Prism, GraphPad software, USA) was determined by incubating the enzymes (hGR, hTrxR and $hTrxR^{U498C}$) for 10 min with NADPH (100 or 200 μM) and inhibitor (0.5–500 nM and 1–40 μM) at 25 °C. The enzyme activity measurement was started by adding GSSG (100 μM), DTNB (3 mM), or hTrx (20 μM) to the mixtures.

2.13. Statistics

Data were analyzed for statistical significance using an unpaired Student's *t*-test. P-values <0.05 were considered to be statistically significant.

3. Results and discussion

3.1. Synthesis and crystal structure of GoPI-sugar

In order to increase the stability and solubility of GoPI, a sugar-linked form of GoPI (1-phenyl-bis(2-pyridyl)phosphole gold chloride thio-β-D-glucose tetraacetate, GoPI-sugar) was synthesized. The modified gold complex **2** (Fig. 1) bearing the 1-phenyl-bis(2-pyridyl)phosphole ligand was readily prepared by reacting the precursor **1** with 1-thio-β-D-glucose tetraacetate in the presence of sodium hydride (Fig. 1B). The novel derivative **2** was isolated as an air-stable yellow powder with 70% yield following purification by column chromatography. Its multinuclear NMR data and mass spectrum support the proposed structure. For example, its $^{31}P\{^1H\}$ NMR chemical shift at +47.3 ppm is typical for Au(I)–phosphole complexes (e.g. **1**, +39.9 ppm). It is worth noting that replacing the Cl ligand with the thio-sugar donor (**1** → **2**, Fig. 1B) results in improved air and moisture stability along with an increase in the solubility properties of the gold complexes. For example, complex **2** is stable in CH_2Cl_2 solution in air for weeks, whereas derivative **1** decomposes within a few hours under the same conditions. Likewise, complex **2** is highly soluble in pentane, whereas **1** is not soluble in this apolar aliphatic solvent. Complex **2** was also characterized by X-ray diffraction studies performed on single crystals (Fig. 1C). The metric data of the 1-phenyl-2,5-bis(2-pyridyl)phosphole ligand are unremarkable and compare well to those of complex **1**. The P–Au distance (2.253(2) Å) as well as the P–Au–S angle (178.28(10)°) are similar to those encountered in phosphole–Au(I) complexes. The Au–S bond distance

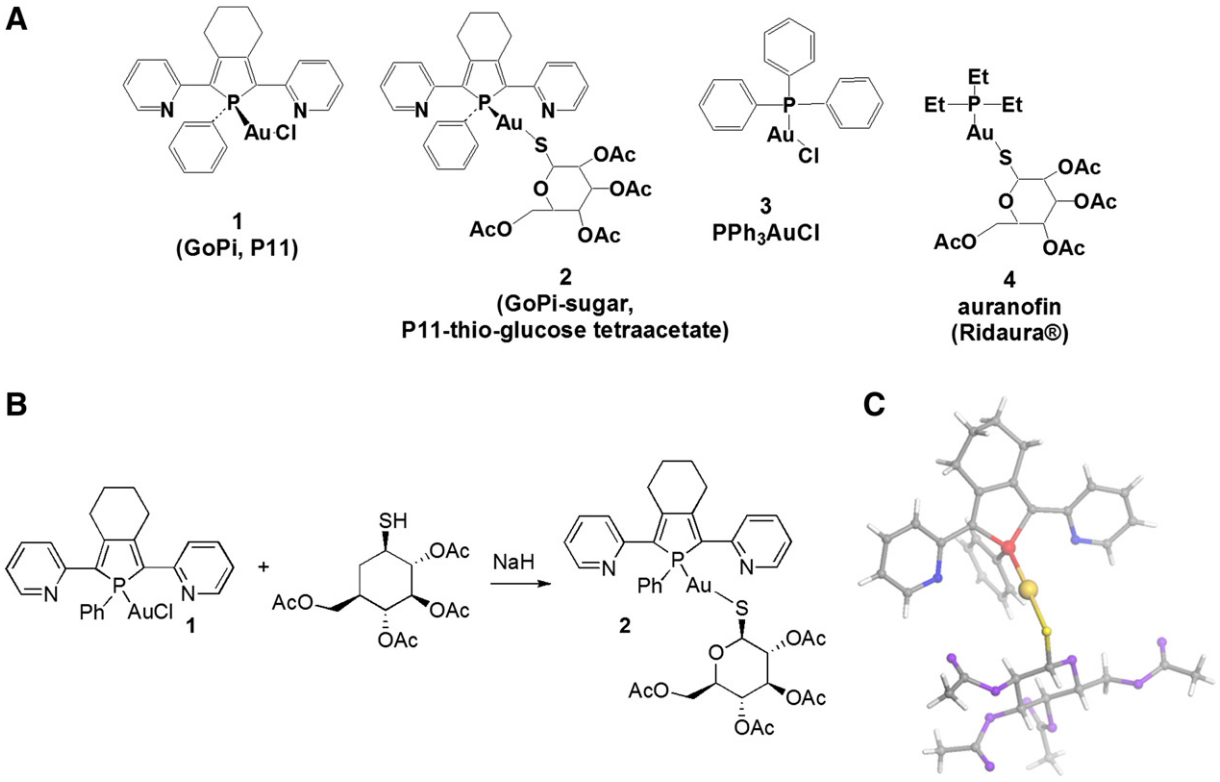

Fig. 1. Structure (A) and synthesis (B) of gold-based compounds. Part (C) shows the crystal structure of complex **2**.

(2.291(2) Å) lies in the range of classic values. Overall, this solid state confirms the proposed structure and reveals no unexpected features.

3.2. GoPI-sugar shows less direct interactions with DNA than GoPI

GoPI was shown to interact with DNA in previous experiments thereby potentially interfering with DNA replication and transcription [3]. To study the DNA-binding behavior of GoPI-sugar, we treated a linearized plasmid DNA with GoPI-sugar and recorded the thermal denaturation of the complex via UV absorption. The DNA melting curves of related metallophospholes were compared to those of related phosphines: GoPI **1**, GoPI-sugar **2**, auranofin **4**, and the commercially available lipophilic Ph_3PAuCl **3** at concentrations between 0 and 10 μM (Fig. 2A). In the drug–DNA interaction study, we mainly investigated the effect of the leaving group attached to the gold phosphine moiety of the molecule. Hence, the comparison between GoPI and GoPI-sugar was obviously guided by the evaluation of the impact of the presence of a good leaving group, i.e. the chlorine atom, versus

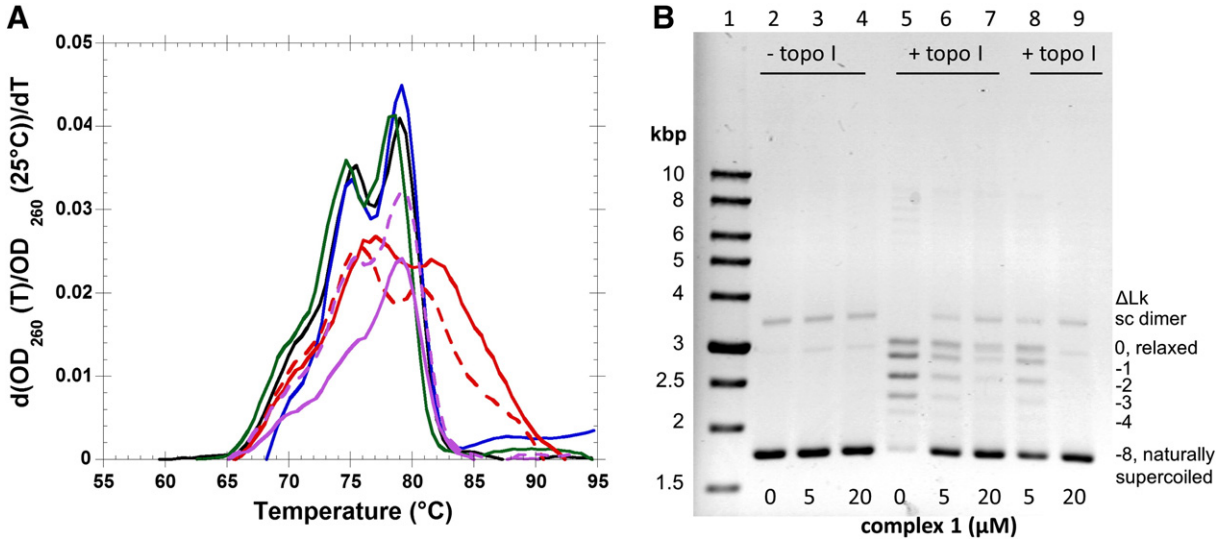

Fig. 2. (A) Effect of gold-based compounds on thermal stability of linearized plasmid DNA. The derivative melting curves are shown for untreated DNA as a control (black) and for DNA in the presence of 5 μM (dashed line) or 10 μM (continuous line) of the compounds (complex **1**: magenta; complex **2**: blue; complex **3**: red; complex **4**: green). (B) Gel-shift assay for testing DNA intercalation of complex **1**. Lane content: DNA size-markers: 1; increasing complex **1** concentration (0–20 μM) in the absence of topoisomerase I: 2–4; in the presence of calf thymus topoisomerase I: 5–7; in the presence of wheat germ topoisomerase I: 8–9. A gradual upwards shift in the topoisomer distribution of the bands was observed at increasing concentrations of complex **1** in the presence of either topoisomerases.

Please cite this article as: E. Jortzik, et al., Antiglioma activity of GoPI-sugar, a novel gold(I)–phosphole inhibitor: Chemical synthesis, mechanistic studies, and effectiveness *in vivo*, Biochim. Biophys. Acta (2014), http://dx.doi.org/10.1016/j.bbapap.2014.01.006

the thiosugar moiety. Previous studies [25] have demonstrated that (i) both gold coordination complexes, auranofin **4** and the related gold(I) chlorotriethyl phosphine, did not induce any observable changes in the electrophoretic mobility of any forms of DNA, when tested with superhelical or relaxed DNA [50,51]; (ii) interaction of auranofin **4** or gold(I) chlorotriethyl phosphine led to the formation of the same gold(I)–DNA complex [30] thereby proving a prodrug effect for auranofin since bioactivation of both compounds leads to the same DNA adduct; (iii) the phosphine-coordinated gold(I) thiosugar complexes displayed higher cytotoxicity *in vitro* and higher antitumor activity *in vivo* when compared to the phosphine-coordinated chloro gold(I) complexes [25]; (iv) the phosphine-coordinated chloro gold(I) complexes Ph_3PAuCl and Et_3PAuCl displayed similar antitumor properties in vivo with the same increase in median life span (ILS) relative to the control P388 leukemia tumor-bearing mice (ILS = 36% for Ph_3PAuCl or Et_3PAuCl versus 70% for auranofin). Therefore, we conducted DNA binding experiments with four drug representatives: both gold(I) chloro- and thio-substituted phosphines. In addition, we selected the commercially available Ph_3PAuCl as a representative of the unavailable Et_3PAuCl in order to compare it to Et_3PAu–thiosugar (auranofin) in our DNA binding studies.

The melting derivative curve of this DNA was composed of two regions: the opening of an AT-richer domain at 75 °C and a GC-richer domain at 79 °C. Contrary to earlier studies with GoPi [3], GoPI-sugar has no significant effect on DNA stability at these concentrations, which is similar to the related compound auranofin. This observation was expected, because GoPI-sugar and auranofin are more stable prodrugs when compared to GoPI due to the nature of their leaving group (thiosugar versus chlorine atom). A similar behavior was previously reported for auranofin and its chloro analog Et_3PAuCl towards DNA interaction, i.e. the absence of DNA interaction for the thiosugar derivative [51]. Melting Ph3PAuCl-treated DNA shows a concentration-dependent stabilization with the effect being somewhat different from that of GoPI: the first melting derivative peak (around 75 °C) related to the denaturation of the AT-rich regions is more affected. In the case of GoPI, both domains were stabilized proportionally to the drug concentration (Fig. 2A).

According to thermal denaturation measurements, some gold complexes stabilize the DNA double helix; however, GoPI-sugar and auranofin only do so to a lesser extent. Various DNA-drug binding modes, which can be distinguished by different techniques, may cause such stabilization. In order to investigate the mode of DNA interaction by the four gold(I) complexes **1**–**4**, we used a gel-shift assay based on topoisomerase I treatment of superhelical DNA in the presence of the drugs (Fig. 2B). This technique relies on the fact that, upon intercalation, the number of superhelical turns in a plasmid changes, and the variations can be monitored by topoisomerase I relaxation. As expected, complexes **2** and **4** did not show any significant interaction, in agreement with previous observations for auranofin [30]. The absence of significant changes with the thio-gold complex **2** in the electrophoretic mobility of any forms of DNA is due to the fact that both, the slow reacting GoPI-sugar **2** and the fast reacting GoPI **1**, are prodrugs and require a bioactivation process to form the same final DNA adducts *in vivo*, as it was previously evidenced for auranofin [30]. Interestingly, we observed that all investigated gold complexes inhibited topoisomerase I. Fig. 2B presents this inhibition for compound 1 depending on the drug concentration. Consequently, DNA intercalation could not be measured unambiguously. We observed this inhibition effect with topoisomerase I from two different sources (animal and plant). Noteworthy, inhibition of human topoisomerase I and II has also been reported for gold(III) complexes of pyridyl- and isoquinolylamido ligands [52] and cyclometalated gold(III) complexes, which also inhibit the growth of different human cell lines [53]. Since this property is interesting in further optimization of GoPI-sugar, it will be studied by topoisomerase inhibition assays in future experiments.

3.3. GoPI-sugar exhibits an antiproliferative effect on glioma cells and reduces in vivo tumor growth of malignant gliomas

In order to analyze the influence of GoPI-sugar on cell proliferation and compare it to GoPI, we measured changes in DNA synthesis by incorporating 5-bromo-2′-deoxy-uridine (BrdU) into human (NCH89, NCH82) and rat (C6) glioma cell lines after treatment with GoPI-sugar. In all three of these cell lines, GoPI-sugar induced a pronounced decrease of tumor cell growth compared to solvent-treated controls. GoPI-sugar inhibited tumor cell growth with EC_{50} values of 0.9 μM (NCH82), 1.5 μM (NCH89) and 1.2 μM (C6), respectively (Fig. 3). Thus, GoPI-sugar inhibits not only human breast cancer cells [41] but also the growth of a glioma cell line with EC_{50} values in a low micromolar range. Interestingly, when compared to GoPI [3], antiproliferative effect on glioma cell lines was increased by 2–12 times by the introduction of a thiosugar, thereby representing a major improvement of the compound. For comparison, it should be mentioned that carmustine (BCNU), an established nitrosourea compound for the treatment of glioblastomas, inhibits the proliferation of these human glioblastoma cell lines with an EC_{50} of 430 μM [3].

In order to study the influence of GoPI-sugar on malignant glioma growth *in vivo*, we employed the C6 glioma rat model that shares important characteristics with human glioblastomas. Animals were treated on day 3, 5, 7, and 9 post-implantation with either a low dose (22 mg/kg body weight), a high dose (30 mg/kg) or a vehicle alone. Tumor size and localization were assessed by representative coronal T_2- and T_1-weighted contrast-enhanced MRI images. Treatment with GoPI-sugar significantly reduced mean tumor volumes by 65% (22 mg/kg body weight) and 88% (30 mg/kg body weight) on day 16 when compared to the control (Fig. 4). Thus, treatment with GoPI-sugar leads to a considerable decrease in the growth of malignant gliomas in rats, demonstrating its *in vivo* efficacy.

3.4. Gold detection in tumor tissue

Using atomic absorption spectroscopy we exemplarily determined the concentrations of gold in the tumor tissue of rats after glioma cell implantation and treatment with 30 mg/kg body weight of GoPI-sugar. In untreated control rats, gold was not detectable in brain tumor tissue. The tumor tissue of rats treated with 30 mg/kg of GoPI-sugar contained 658.5 ng/g gold in the contralateral hemisphere and 804.7 ng/g gold in the tumor-bearing hemisphere. This indicates that GoPI-sugar, or at least the gold moiety, indeed crossed the blood–brain barrier and reached the brain tissue at relevant levels with some preference for the glioblastoma tumor cells.

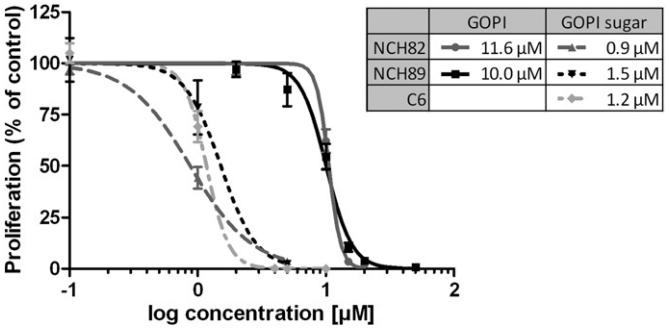

Fig. 3. Antiproliferative effects of GoPI-sugar and GoPI on two human (NCH89, NCH82) and a rat (C6) glioma cell line by GoPI-sugar and GoPI. Corresponding EC_{50} values are given in the table.

Please cite this article as: E. Jortzik, et al., Antiglioma activity of GoPI-sugar, a novel gold(I)–phosphole inhibitor: Chemical synthesis, mechanistic studies, and effectiveness *in vivo*, Biochim. Biophys. Acta (2014), http://dx.doi.org/10.1016/j.bbapap.2014.01.006

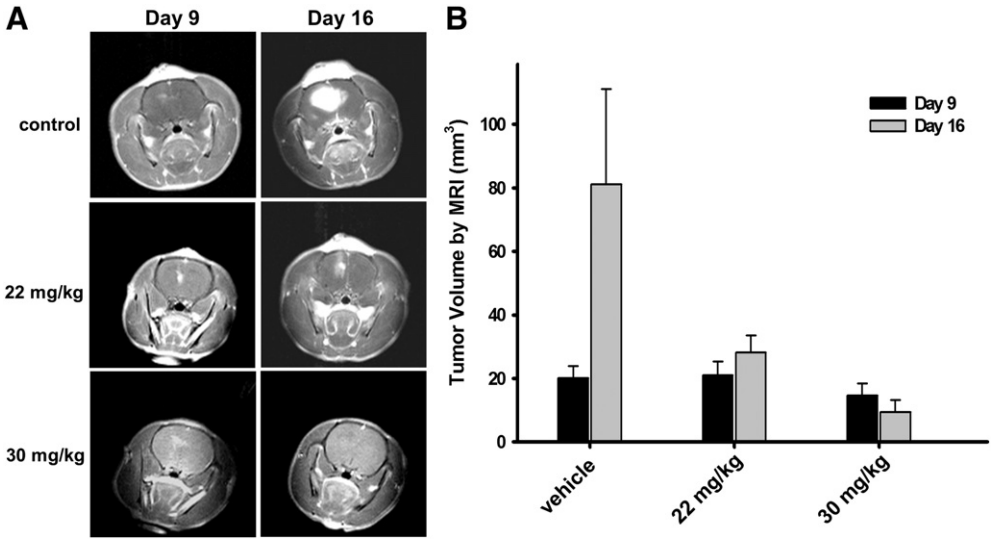

Fig. 4. Effect of GoPI-sugar on a C6 glioma model. Part (A) shows a representative Magnevist enhanced T_1-weighted MRI image from each treatment group on days 6 and 16 after cell implantation. Part (B) shows the tumor volume of the treatment groups compared to the controls on days 6 and 16.

3.5. GoPI-sugar displays a low toxicity towards C6 rats

GoPI-sugar treatment was generally well tolerated and did not lead to histopathological alterations in the vital organs including the liver, lung, kidney, skin, gut, heart, muscle, pancreas, and spleen. The body weight of C6 glioma-bearing rats showed no significant differences between either of the treatment groups and the control group, with a mean weight of 237 ± 25 g on day 0 and 282 g ± 27 g on day 16 (treated animals) compared to 251 ± 33 g and 281 ± 26 g (control animals). Within a few hours after the first application, two animals of the treatment group and one animal of the control group died. The absence of histopathological alterations with a clinically acute occurrence of cardiopulmonary decompensation most likely indicates a toxic shock with anaphylaxis. However, a pulmonary embolism cannot be excluded. Analysis of different blood parameters showed no significant changes in both groups. There were mild but insignificant differences in hepatic function parameters with elevated serum glutamate oxaloacetate transaminase (GOT) and decreased cholinesterase (CHE) levels in treated animals. Significant changes in renal function parameters and blood counts were not observed (Table 1).

3.6. Reduced tumor growth is caused by downregulation of tumor cell proliferation but not due to an induction of apoptosis

Tumor sections from treated and control animals were employed to assess cell proliferation via Ki-67 staining. In animals treated with a high dose (30 mg/kg body weight) of GoPI-sugar, we observed a significantly decreased tumor cell proliferation by 59% (Fig. 5), while 20 mg/kg did show an antiproliferative effect. This was, however, not significant and corresponds to the fact that no gold could be detected in the brain tumor tissue of rats treated with a low dose as reported in Section 3.4. To further explore whether reduced tumor cell proliferation is associated with increased apoptosis, we applied TUNEL staining on neighboring tumor sections. Interestingly, we did not detect a significant increase in the number of apoptotic cells in tumor tissue of GoPI-sugar-treated rats (Fig. 6), indicating that GoPI-sugar does not induce apoptosis at the concentrations examined. However, it cannot be excluded that anti-apoptotic effects were not anymore detectable, because treatment ended on d9 while the analysis was performed on post-mortem brains from d16. Contrarily, GoPI-sugar treatment increased nuclear fragmentation and chromatin condensation in human breast cancer cells (MCF-7) [41]. This might point towards a different mode of cell death in brain

Table 1
Stability of metabolic parameters in the blood of rats treated with GoPI-sugar (d16). The values indicate very low acute in vivo drug toxicity of the compound.

	Control	GoPI-sugar (22 mg/kg)	GoPI-sugar (30 mg/kg)	
Cr	0.2 ± 0.1	0.3 ± 0.0	0.3 ± 0.1	mg/dL
BUN	29.3 ± 10.4	33.7 ± 5.3	30.8 ± 4.8	mg/dL
GOT	65.6 ± 3.7	143.5 ± 73.3	117 ± 85.2	U/L
GPT	37 ± 6.2	51.2 ± 7.6	51.2 ± 11.7	U/L
AP	121.6 ± 70.8	128.2 ± 62.8	170.8 ± 47.3	U/L
GGT	1.3 ± 3.0	2.2 ± 0.5	1.4 ± 1.9	U/L
CHE	0.4 ± 0.3	0.4 ± 0.4	0.2 ± 0.0	kU/L
Bilirubin	0.2 ± 0	0.2 ± 0	0.1 ± 0.0	mg/dL
Hb	14.6 ± 1.3	11.8 ± 0.3	12.7 ± 1.2	g/dL
RBC	6.8 ± 0.4	6.4 ± 0.2	6.1 ± 0.2	/pL
Hk	0.4 ± 0.0	0.3 ± 0.0	0.3 ± 0.0	l/L
WBC	5.9 ± 2.1	10.8 ± 0.7	7.9 ± 4.6	/nL
Platelet	1264 ± 500.6	1297 ± 33.2	1227 ± 230.7	/nL

CHE, cholinesterase; Cr, creatinine; BUN, blood urea nitrogen; GGT, gamma-glutamyl transpeptidase; GOT, serum glutamate oxaloacetate transaminase; GPT, serum glutamate pyruvate transaminase; AP, alkaline phosphatase; RBC, red blood cells; Hb, hemoglobin; Hk, hematocrit; WBC, white blood cells.

Please cite this article as: E. Jortzik, et al., Antiglioma activity of GoPI-sugar, a novel gold(I)–phosphole inhibitor: Chemical synthesis, mechanistic studies, and effectiveness *in vivo*, Biochim. Biophys. Acta (2014), http://dx.doi.org/10.1016/j.bbapap.2014.01.006

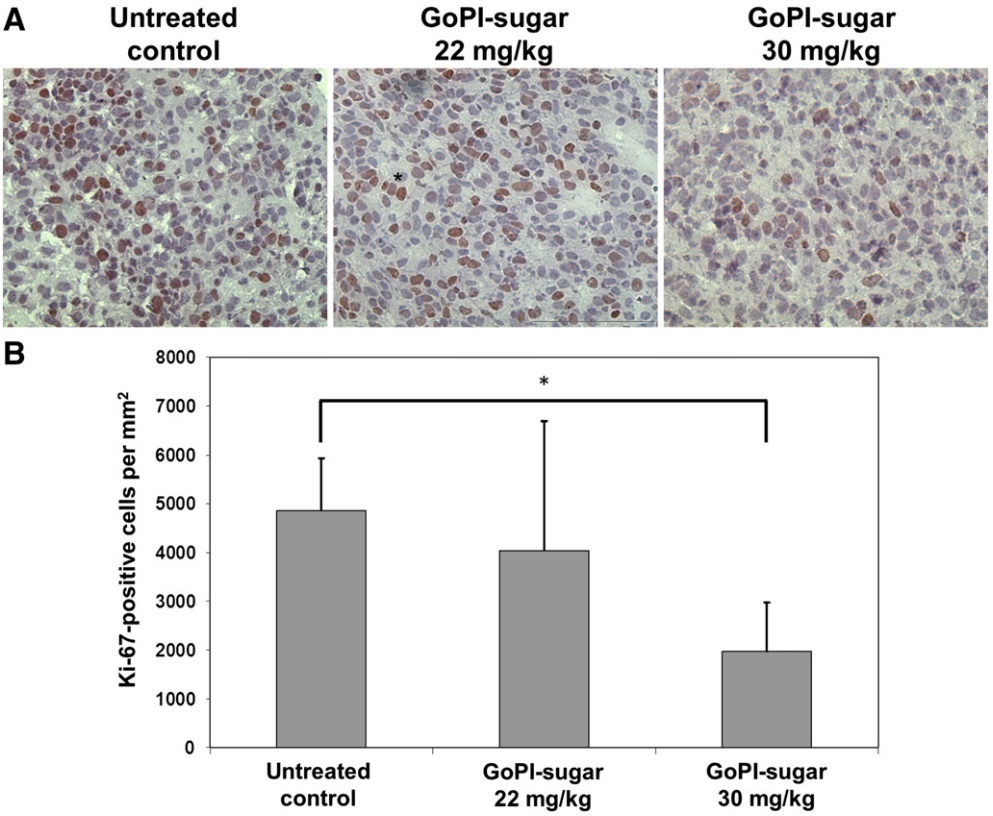

Fig. 5. Tumor cell proliferation after treatment with GoPI-sugar (d16). (A) Tumor sections from each of the groups were examined by immunohistochemistry for cell proliferation by using a Ki-67 antibody. (B) Quantitative analyses of the percentage of proliferating cells in GoPI-sugar-treated tumors and controls. Positive cells were counted in three hotspots per tumor sample. A comparison of Ki-67-positive cells in tumor sections (5 μm) shows that treatment with 30 mg GoPI-sugar/kg, but not with 22 mg GoPI-sugar/kg, significantly inhibits primary tumor cell proliferation. *$P < 0.005$.

tumors and breast tumors or is more likely due to different compound concentrations and consequently different effects in tumor tissue *in vivo* and in cell culture. Antiproliferative effects with induction of apoptosis by gold(I) compounds have been demonstrated in different cancer cell lines: Gold(I) complexes of imidazole and thiazole-based diphos type ligands induced DNA fragmentation in the hepatic tumor cell line H4IIE [40], and different phosphine gold(I) complexes were shown to activate caspase-3 and capase-9 and induce apoptosis in cancer cells [6,54]. Therefore, the effect of GoPI-sugar on cell death has to be studied systematically.

3.7. Inhibition of recombinant redox enzymes by GoPI-sugar

To test the interaction between recombinant redox enzymes and GoPI-sugar, we measured the half-maximal inhibition induced by 10 min incubation of the prereduced enzymes with GoPI-sugar on recombinant human GR, human TrxR isolated from placenta, and the recombinant selenocysteine-lacking mutant $hTrxR^{U498C}$ *in vitro* (Table 3, Fig. 7). The data can be directly compared to the values previously reported for GoPI (Table 3, [3]). Under the conditions chosen, GoPI-sugar inhibits human GR with an IC_{50} of 88.5 nM, and is thus less efficient than GoPI which inactivated the enzyme at an almost stoichiometric concentration of 2 nM [3]. In good accordance, auranofin, a phosphine-coordinated gold(I) thiosugar complex, does not show a pronounced inhibition of hGR [55], indicating that the presence of a thiosugar moiety decreases the affinity of the inhibitor for hGR. Eventually, the access of the enlarged inhibitor to the active site of GR and the subsequent attack of residue Cys58 leading to the formation of a (Cys58–S)–Au–phosphole intermediate might be hindered by the thiosugar. After successful access, the thioglucose might be replaced by the dithiol target as reported for auranofin [41]. However, combining GoPI with a thiosugar slightly improved hTrxR inhibition, which is reflected by an IC_{50} of 4.3 nM for GoPI-sugar compared to 7 nM for GoPI as determined in the Trx-assay (Table 3, Fig. 7). This result might be reflected in the improved antiproliferative activity of GoPI-sugar as discussed in Section 3.3. Since the Sec→Cys mutant of hTrxR ($hTrxR^{U498C}$) is much less affected by GoPI-sugar than the wild type enzyme (more than two orders of magnitude in both the DTNB and the Trx-assay), the major primary site of GoPI-sugar action seems to be the reactive selenocysteine residue at the C-terminal active site of hTrxR. In hTrxR (or *S. mansoni* TGR) the selenocysteine residue has been shown to be involved in the transfer of gold from phosphine ligands in GoPI complexes to the redox-active Cys pair of the enzymes. In TGR catalysis, a transient intermediate bearing an Au(I) coordinated with Sec597 and triethylphosphine, upon the prior release of acetoxythioglucose, has been proposed. Subsequently, the intermediate species releases triethylphosphine to form a Sec-gold-Cys complex with any of the available cysteinyl residues, which can rearrange to yield the more stable short-distance Cys–gold–Cys complexes when equilibrium is reached [31]. As studied in detail by Urig et al. 2006 [3], the inhibition pattern of disulfide reductases by goldphospholes seems to be very complex and can be described by an initial competition with the oxidizing substrate followed by an irreversible reaction leading to covalently modified enzyme. Also the substoichiometric inhibition of hTrxR which became very evident in our studies on GoPI-sugar had already been reported in Urig et al. for GoPI [3]. Although the underlying mechanism is not fully understood, we hypothesize that this substoichiometric inhibition is based on various overlaying effects which include: (i) interaction of substrates and inhibitors with both N-terminal and C-terminal active sites; (ii) competitive (reversible) and covalent (irreversible) inhibition; and (iii) most of all, enhanced instability of hTrxR in the presence of NADPH and inhibitor which becomes critical over the incubation time of 10 min.

Please cite this article as: E. Jortzik, et al., Antiglioma activity of GoPI-sugar, a novel gold(I)–phosphole inhibitor: Chemical synthesis, mechanistic studies, and effectiveness *in vivo*, Biochim. Biophys. Acta (2014), http://dx.doi.org/10.1016/j.bbapap.2014.01.006

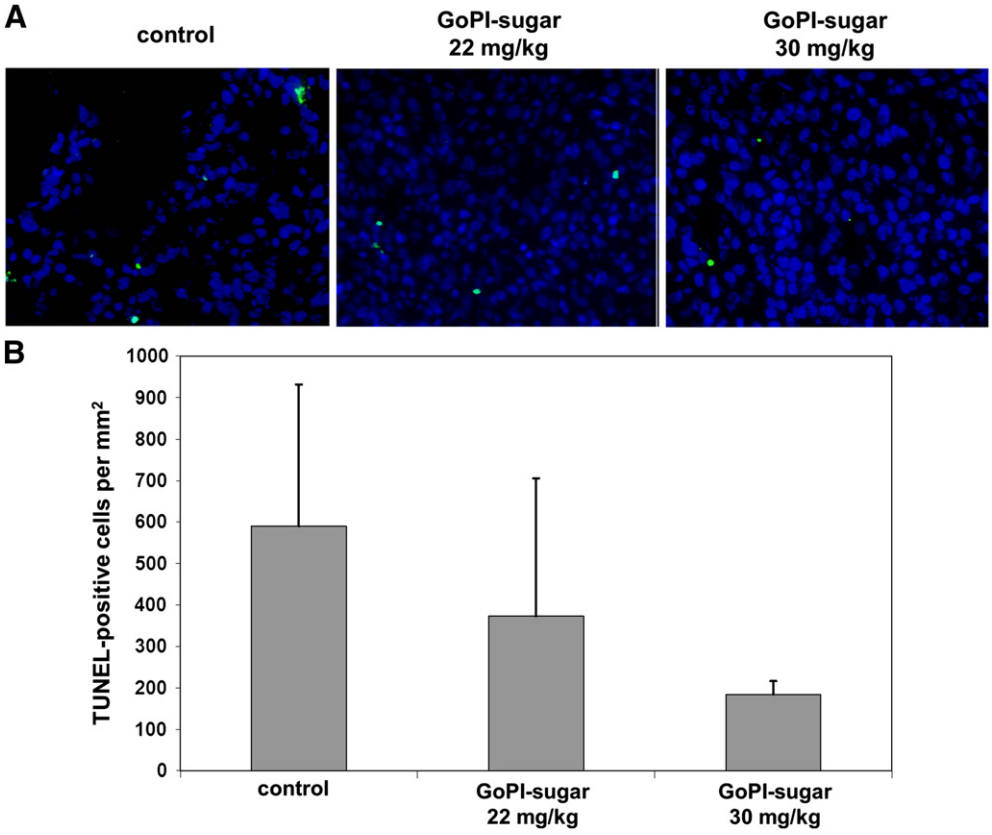

Fig. 6. Apoptosis in tumor sections from C6 glioma rats (d16) treated with GoPI-sugar and untreated controls. (A) Tumor sections from each of the groups were examined using TUNEL staining. (B) Quantitative analysis of apoptotic cells per mm^2 in treated tumors and controls. Positive cells were counted in three hotspots per tumor sample. A comparison of TUNEL-positive cells per mm^2 shows no significant difference between treated and untreated tumors.

3.8. Tissue-specific variation of redox parameters after GoPI-sugar treatment

Different gold(I) complexes including GoPI were shown to affect the redox system of cancer cells by inhibiting thioredoxin reductase and/or glutathione reductase via their active site thiols [3,4,6,8]. In order to systematically address the effect of GoPI-sugar treatment on the redox status of C6 glioma rats, we measured the activities of central redox enzymes such as TrxR, GPx, GR, and GST, as well as concentrations of total glutathione in the blood, five different rat tissues including the brain of C6 glioma rats treated with GoPI-sugar, and untreated control animals. Data are summarized in Table 2. Interestingly, total glutathione concentrations were only significantly reduced in the kidney, while the other organs including the brain showed no significant alterations in total glutathione concentration. Moreover, healthy brain and brain tumor tissue from rats contain the same levels of glutathione. On the contrary, Kudo et al. [56] determined significantly decreased glutathione levels in glioblastoma compared to normal human brain tissue (195 μg/g and 444 μg/g, respectively). However, total glutathione concentrations do not give any information on the glutathione redox potential. Examining changes in the ratio of reduced to oxidized glutathione (e.g. by genetically encoded probes) will allow a more precise statement on the redox state of the cells following GoPI-sugar treatment.

GST activity was significantly increased in the blood of rats treated with GoPI-sugar. The observed upregulation of GST most likely occurs due to increased drug pressure. GSTs are phase II enzymes that detoxify xenobiotics including anticancer drugs by conjugating the molecules with GSH, which are subsequently exported from the cell. GSTs have been implicated in resistance against cancer therapeutics and the lacking clinical response of brain tumors. The major isoform in brain tissue, GST π, was reported to be elevated in malignant tumors [57]. A high expression of GST π is associated with a shorter survival time of glioma patients and is related to more aggressive and/or chemoresistant tumors [58]. Upon treatment with certain anticancer agents, the expression of different GST isoforms in human brain tumors is induced [19]. However, GoPI-sugar treatment did not influence the levels of GST activity in brain tumor tissue in our rat glioma model (Table 2), pointing towards a different mode of action and a lower probability of resistance development against GoPI-sugar, an aspect that is worth studying in detail.

The activities of the selenoproteins TrxR and GPx were reduced in most tissues after treatment with GoPI-sugar, however, not significantly. Significantly higher TrxR activities in GoPI-sugar-treated rats compared to untreated controls were observed in the kidney and liver, which might be due to compensatory upregulation of the enzymes in these organs involved in detoxification, metabolization, and excretion of xenobiotics. Interestingly, contrary to the fact that GoPI-sugar inhibits hTrxR with an IC_{50} of 4.3 nM *in vitro* (Section 3.7), brain tumor tissue did not show any decrease in TrxR activity after treatment. Again, this result might be due to a stimulation of TrxR activity under drug treatment leading to a compensatory upregulation of transcription in parallel to the inhibition. A similar phenomenon has been observed previously when TrxR activity was determined in glioblastoma cells treated with terpyridine platinum complexes as TrxR inhibitors [43]. Notably, in our experiments, TrxR activity was significantly lower in untreated rat brain tumors when compared to untreated healthy brains (Table 2). This is a somewhat unexpected finding, since different human tumor cell lines have elevated expression levels and/or increased activity of TrxR and Trx such as human lung adenocarcinoma cells [59], human colorectal tumors, breast cancer cells [60], and thyroid cancer cells [61], promoting tumor growth and progression. Similarly,

Please cite this article as: E. Jortzik, et al., Antiglioma activity of GoPI-sugar, a novel gold(I)–phosphole inhibitor: Chemical synthesis, mechanistic studies, and effectiveness *in vivo*, Biochim. Biophys. Acta (2014), http://dx.doi.org/10.1016/j.bbapap.2014.01.006

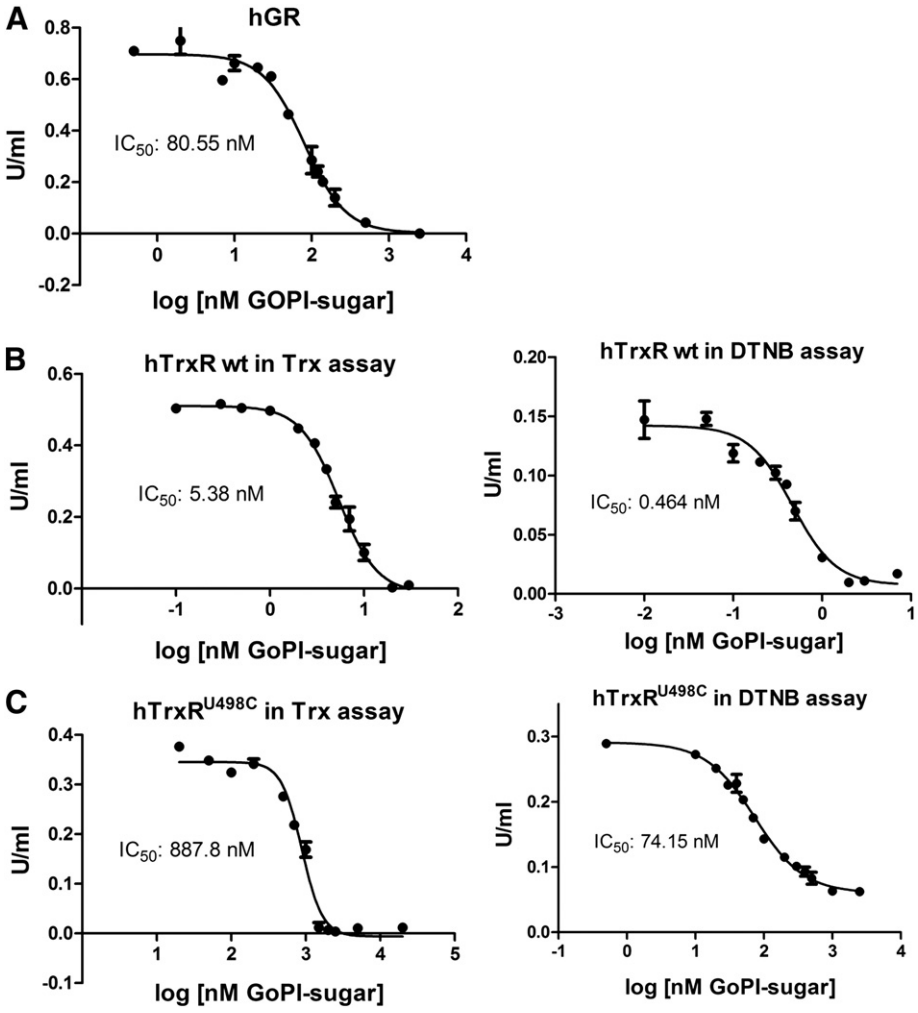

Fig. 7. Inhibition studies with GoPI-sugar on hGR (A), hTrxR wild type (B) and hTrxRU498C (C). For hTrxR, the inhibition has been tested by using both thioredoxin and DTNB as a substrate. One representative graph of each IC_{50} determination is shown.

TrxR activity in glioblastoma tissue from human patients was found to be significantly higher than in the control group (74.5 U/g wet tissue and 14.8 U/g wet tissue, respectively) [62]. The comparatively low TrxR activity in the tumor cells studied here might indicate a higher variability of glioblastoma cells than originally expected. However, concerning its therapeutic effects, the GoPI-sugar with its high affinity for TrxR is likely to be even more effective in tumor cells with upregulated TrxR activity.

In our *in vivo* study, the investigated redox parameters in brain tissue were hardly affected by the treatment. This might partially be explained by compensatory upregulation of redox-related enzymes. However, based on these results, it can be assumed that the inhibition of brain tumor growth by GoPI-sugar is based on its increased stability with respect to nucleophiles and on its DNA intercalating properties rather than on the inhibition of redox enzymes. As previously investigated [63], the high affinity of gold(I) for sulfur and selenium ligands

Table 2
Redox parameters in different tissues of C6 glioma rats after treatment with GoPI-sugar (30 mg/kg, d16).

	Group	Brain tissue	Brain tumor	Kidney	Muscle	Liver	Blood
Glutathione (mM)	Control	0.3 ± 0	0.3 ± 0	0.3 ± 0.1	0.4 ± 0.1	2.9 ± 0.5	1.1 ± 0.4
	Treated	0.4 ± 0.1	0.3 ± 0.1	0.1 ± 0*	0.5 ± 0.1	2.2 ± 0.7	1.1 ± 0.4
TrxR (mU/mg protein)	Control	26.7 ± 0	18.3 ± 1.2	28.7 ± 1.3	17.4 ± 7.0	26.5 ± 5.9	n.d.
	Treated	24.6 ± 4.9	19.9 ± 4.1	11.1 ± 4*	13.6 ± 1.5	17.1 ± 1.8*	n.d.
GR (mU/mg protein)	Control	59.6 ± 0	79.9 ± 8.9	30.6 ± 17	17.5 ± 6.3	115 ± 20.7	16.1 ± 12.2
	Treated	61.9 ± 10	83.2 ± 21	36.1 ± 6.7	22.5 ± 7.5	103 ± 14.4	16.9 ± 0
GPx (mU/mg protein)	Control	74.2 ± 0	96.5 ± 11	630 ± 57.9	117 ± 57.3	869 ± 369	381 ± 59.6
	Treated	71.1 ± 5.8	104 ± 55.7	568 ± 187	86.7 ± 10	485 ± 70.5	468 ± 199
GST (mU/mg protein)	Control	131 ± 0	131 ± 20.6	31.1 ± 8.8	39.5 ± 17	317 ± 51	6.9 ± 1.5
	Treated	122 ± 25.1	195 ± 216	26.4 ± 5.6	23.3 ± 2.2	353 ± 20.3	10.5 ± 0.9*

c — untreated control: n = 3 except in healthy brain (n = 1).
t — treated with 30 mg GoPI-sugar/kg body weight: n = 5 except in healthy brain (n = 4) and muscle (n = 3).
n.d. — not determined.
* Significant differences between untreated and treated animals ($p < 0.05$).

Please cite this article as: E. Jortzik, et al., Antiglioma activity of GoPI-sugar, a novel gold(I)–phosphole inhibitor: Chemical synthesis, mechanistic studies, and effectiveness *in vivo*, Biochim. Biophys. Acta (2014), http://dx.doi.org/10.1016/j.bbapap.2014.01.006

Table 3
Half-maximal inhibition of disulfide reductases by GoPI and GoPI-sugar after 10 min preincubation of the NADPH-reduced enzymes with inhibitor.

Enzyme	Oxidizing substrate	$IC_{0.5}$ [nM]	
		GoPI[a]	GoPI-sugar
hGR	GSSG	2	88.5 ± 28
hTrxR	$hTrx^{C72S}$	7	4.3 ± 1.6
	DTNB	1	0.49 ± 0.04
$hTrxR^{U498C}$	$hTrx^{C72S}$	1900	834.9 ± 74.8
	DTNB	3000	66.8 ± 5.8

[a] Values as reported in Ref. [3].

suggests that gold thiosugar will be displaced by proteins in the blood, including redox enzymes and transport proteins, and be primarily bound to proteins as part of the mechanism of protein-mediated transport of gold to the final targets during therapy.

4. Conclusion

Gold compounds exhibit a high affinity for sulfur- and selenium-containing ligands such as proteins with selenocysteine as exposed active site residues. By combining gold(I) with a nucleophilic phosphole ligand with limited aromatic character, the reactivity with thiol-containing proteins is even more pronounced [3,4]. Here, we show that a (phosphole)gold chloride complex linked to a thiosugar inhibits the growth of a glioma cell line with IC_{50} values in a low micromolar range. Interestingly, introducing the sugar residue did improve the solubility of GoPI-sugar and its antiproliferative effect when compared to GoPI, thereby representing a major improvement of the compound. Treatment of C6 rats bearing malignant glioblastomas with GoPI-sugar was well tolerated and led to a drastic decrease in tumor growth. In contrast to previous studies on gold(I) complexes, targeting the thioredoxin system and disturbing the redox system in cancer cells does not seem to be the major mode of action of GoPI-sugar, since the activities of hTrxR and other redox parameters were only slightly altered in the brains of the treated animals. Our observations rather point towards inhibition of DNA replication via the interaction of GoPI-sugar with DNA, and/or inhibition of topoisomerase I, features that deserve to be studied in more detail. Due to its high efficacy against glioblastomas *in vivo* and its low toxicity, GoPI-sugar is a promising lead compound for future anticancer therapies.

Acknowledgements

The authors thank Radoslav Enchev for the DNA binding studies and Marina Fischer for her excellent technical assistance. Parts of this work were supported by the Deutsche Forschungsgemeinschaft (BE 1540/11-2 to K.B. and JO 1085/1-2 to E.J.), by the Centre National de la Recherche Scientifique, France (CNRS, France, UMR 7509 [E.D.–C.]), and the Laboratoire d'Excellence (LabEx) ParaFrap (grant LabEx ParaFrap ANR-11-LABX-0024 [E.D.–C.]).

Appendix A. Supplementary data

Supplementary data to this article can be found online at http://dx.doi.org/10.1016/j.bbapap.2014.01.006.

References

[1] P.C. Bruijnincx, P.J. Sadler, New trends for metal complexes with anticancer activity, Curr. Opin. Chem. Biol. 12 (2008) 197–206.
[2] S. Komeda, A. Casini, Next-generation anticancer metallodrugs, Curr. Top. Med. Chem. 12 (2012) 219–235.
[3] S. Urig, K. Fritz-Wolf, R. Reau, C. Herold-Mende, K. Toth, E. Davioud-Charvet, K. Becker, Undressing of phosphine gold(I) complexes as irreversible inhibitors of human disulfide reductases, Angew. Chem. Int. Ed. Engl. 45 (2006) 1881–1886.
[4] M. Deponte, S. Urig, L.D. Arscott, K. Fritz-Wolf, R. Reau, C. Herold-Mende, S. Koncarevic, M. Meyer, E. Davioud-Charvet, D.P. Ballou, C.H. Williams Jr., K. Becker, Mechanistic studies on a novel, highly potent gold-phosphole inhibitor of human glutathione reductase, J. Biol. Chem. 280 (2005) 20628–20637.
[5] E. Vergara, A. Casini, F. Sorrentino, O. Zava, E. Cerrada, M.P. Rigobello, A. Bindoli, M. Laguna, P.J. Dyson, Anticancer therapeutics that target selenoenzymes: synthesis, characterization, in vitro cytotoxicity, and thioredoxin reductase inhibition of a series of gold(I) complexes containing hydrophilic phosphine ligands, ChemMedChem 5 (2010) 96–102.
[6] V. Gandin, A.P. Fernandes, M.P. Rigobello, B. Dani, F. Sorrentino, F. Tisato, M. Bjornstedt, A. Bindoli, A. Sturaro, R. Rella, C. Marzano, Cancer cell death induced by phosphine gold(I) compounds targeting thioredoxin reductase, Biochem. Pharmacol. 79 (2010) 90–101.
[7] R. Galassi, A. Burini, S. Ricci, M. Pellei, M.P. Rigobello, A. Citta, A. Dolmella, V. Gandin, C. Marzano, Synthesis and characterization of azolate gold(I) phosphane complexes as thioredoxin reductase inhibiting antitumor agents, Dalton Trans. 41 (2012) 5307–5318.
[8] E. Schuh, C. Pfluger, A. Citta, A. Folda, M.P. Rigobello, A. Bindoli, A. Casini, F. Mohr, Gold(I) carbene complexes causing thioredoxin 1 and thioredoxin 2 oxidation as potential anticancer agents, J. Med. Chem. 55 (2012) 5518–5528.
[9] A. Holmgren, J. Lu, Thioredoxin and thioredoxin reductase: current research with special reference to human disease, Biochem. Biophys. Res. Commun. 396 (2010) 120–124.
[10] H. Hafsi, P. Hainaut, Redox control and interplay between p53 isoforms: roles in the regulation of basal p53 levels, cell fate, and senescence, Antioxid. Redox Signal. 15 (2011) 1655–1667.
[11] H. Haapasalo, M. Kylaniemi, N. Paunu, V.L. Kinnula, Y. Soini, Expression of antioxidant enzymes in astrocytic brain tumors, Brain Pathol. 13 (2003) 155–164.
[12] G. Powis, D. Mustacich, A. Coon, The role of the redox protein thioredoxin in cell growth and cancer, Free Radic. Biol. Med. 29 (2000) 312–322.
[13] A. Yokomizo, M. Ono, H. Nanri, Y. Makino, T. Ohga, M. Wada, T. Okamoto, J. Yodoi, M. Kuwano, K. Kohno, Cellular levels of thioredoxin associated with drug sensitivity to cisplatin, mitomycin C, doxorubicin, and etoposide, Cancer Res. 55 (1995) 4293–4296.
[14] R.B. Penney, D. Roy, Thioredoxin-mediated redox regulation of resistance to endocrine therapy in breast cancer, Biochim. Biophys. Acta 1836 (2013) 60–79.
[15] M. Selenius, M. Hedman, D. Brodin, V. Gandin, M.P. Rigobello, J. Flygare, C. Marzano, A. Bindoli, O. Brodin, M. Bjornstedt, A.P. Fernandes, Effects of redox modulation by inhibition of thioredoxin reductase on radiosensitivity and gene expression, J. Cell. Mol. Med. 16 (2012) 1593–1605.
[16] S. Urig, K. Becker, On the potential of thioredoxin reductase inhibitors for cancer therapy, Semin. Cancer Biol. 16 (2006) 452–465.
[17] H.W. Lim, S. Hong, W. Jin, S. Lim, S.J. Kim, H.J. Kang, E.H. Park, K. Ahn, C.J. Lim, Up-regulation of defense enzymes is responsible for low reactive oxygen species in malignant prostate cancer cells, Exp. Mol. Med. 37 (2005) 497–506.
[18] J.M. Estrela, A. Ortega, E. Obrador, Glutathione in cancer biology and therapy, Crit. Rev. Clin. Lab. Sci. 43 (2006) 143–181.
[19] D.S. Backos, C.C. Franklin, P. Reigan, The role of glutathione in brain tumor drug resistance, Biochem. Pharmacol. 83 (2012) 1005–1012.
[20] K. Fritz-Wolf, S. Urig, K. Becker, The structure of human thioredoxin reductase 1 provides insights into C-terminal rearrangements during catalysis, J. Mol. Biol. 370 (2007) 116–127.
[21] S.N. Savvides, M. Scheiwein, C.C. Bohme, G.E. Arteel, P.A. Karplus, K. Becker, R.H. Schirmer, Crystal structure of the antioxidant enzyme glutathione reductase inactivated by peroxynitrite, J. Biol. Chem. 277 (2002) 2779–2784.
[22] C. Hay, M. Hissler, C. Fischmeister, J. Rault-Berthelot, L. Toupet, L. Nyulaszi, R. Reau, Phosphole-containing pi-conjugated systems: from model molecules to polymer films on electrodes, Chemistry 7 (2001) 4222–4236.
[23] J.M. Madeira, D.L. Gibson, W.F. Kean, A. Klegeris, The biological activity of auranofin: implications for novel treatment of diseases, Inflammopharmacology 20 (2012) 297–306.
[24] A. Debnath, D. Parsonage, R.M. Andrade, C. He, E.R. Cobo, K. Hirata, S. Chen, G. Garcia-Rivera, E. Orozco, M.B. Martinez, S.S. Gunatilleke, A.M. Barrios, M.R. Arkin, L.B. Poole, J.H. McKerrow, S.L. Reed, A high-throughput drug screen for *Entamoeba histolytica* identifies a new lead and target, Nat. Med. 18 (2012) 956–960.
[25] C.K. Mirabelli, R.K. Johnson, D.T. Hill, L.F. Faucette, G.R. Girard, G.Y. Kuo, C.M. Sung, S.T. Crooke, Correlation of the in vitro cytotoxic and in vivo antitumor activities of gold(I) coordination complexes, J. Med. Chem. 29 (1986) 218–223.
[26] M.T. Coffer, C.F. Shaw, M.K. Eidsness, J.W. Watkins, R.C. Elder, Reactions of auranofin and Et3paucl with bovine serum-albumin, Inorg. Chem. 25 (1986) 333–339.
[27] M.T. Coffer, C.F. Shaw, A.L. Hormann, C.K. Mirabelli, S.T. Crooke, Thiol competition for Et3paus-albumin — a nonenzymatic mechanism for Et3po formation, J. Inorg. Biochem. 30 (1987) 177–187.
[28] J. Christodoulou, P.J. Sadler, A. Tucker, H-1-Nmr of albumin in human blood-plasma — drug-binding and redox reactions at Cys(34), FEBS Lett. 376 (1995) 1–5.
[29] J. Zou, P. Taylor, J. Dornan, S.P. Robinson, M.D. Walkinshaw, P.J. Sadler, First crystal structure of a medicinally relevant gold protein complex: unexpected binding of [Au(PEt3)](+) to histidine, Angew. Chem. Int. Ed. 39 (2000) 2931–2934.
[30] C.E. Blank, J.C. Dabrowiak, Absorption and circular dichroism studies of a gold (I)–DNA complex, J. Inorg. Biochem. 21 (1984) 21–29.
[31] F. Angelucci, A.A. Sayed, D.L. Williams, G. Boumis, M. Brunori, D. Dimastrogiovanni, A.E. Miele, F. Pauly, A. Bellelli, Inhibition of *Schistosoma mansoni* thioredoxin–

glutathione reductase by auranofin: structural and kinetic aspects, J. Biol. Chem. 284 (2009) 28977–28985.
[32] F. Saccoccia, F. Angelucci, G. Boumis, M. Brunori, A.E. Miele, D.L. Williams, A. Bellelli, On the mechanism and rate of gold incorporation into thiol-dependent flavoreductases, J. Inorg. Biochem. 108 (2012) 105–111.
[33] A.N. Kuntz, E. Davioud-Charvet, A.A. Sayed, L.L. Califf, J. Dessolin, E.S. Arner, D.L. Williams, Thioredoxin glutathione reductase from *Schistosoma mansoni*: an essential parasite enzyme and a key drug target, PLoS Med. 4 (2007) e206.
[34] Y. Wang, Y. Wang, X. Chen, Z. Zhang, S. Li, B. Chen, C. Wu, L. Wang, X. Zhang, J. Wang, L. Chen, T. Jiang, Comparison of the clinical efficacy of temozolomide (TMZ) versus nimustine (ACNU)-based chemotherapy in newly diagnosed glioblastoma, Neurosurg. Rev. 47 (2014) 73–78.
[35] R. Stupp, M.E. Hegi, W.P. Mason, M.J. van den Bent, M.J. Taphoorn, R.C. Janzer, S.K. Ludwin, A. Allgeier, B. Fisher, K. Belanger, P. Hau, A.A. Brandes, J. Gijtenbeek, C. Marosi, C.J. Vecht, K. Mokhtari, P. Wesseling, S. Villa, E. Eisenhauer, T. Gorlia, M. Weller, D. Lacombe, J.G. Cairncross, R.O. Mirimanoff, Effects of radiotherapy with concomitant and adjuvant temozolomide versus radiotherapy alone on survival in glioblastoma in a randomised phase III study: 5-year analysis of the EORTC-NCIC trial, Lancet Oncol. 10 (2009) 459–466.
[36] S.J. Berners-Price, A. Filipovska, Gold compounds as therapeutic agents for human diseases, Metallomics 3 (2011) 863–873.
[37] A. Casini, L. Messori, Molecular mechanisms and proposed targets for selected anticancer gold compounds, Curr. Top. Med. Chem. 11 (2011) 2647–2660.
[38] R. Rubbiani, S. Can, I. Kitanovic, H. Alborzinia, M. Stefanopoulou, M. Kokoschka, S. Monchgesang, W.S. Sheldrick, S. Wolfl, I. Ott, Comparative in vitro evaluation of N-heterocyclic carbene gold(I) complexes of the benzimidazolylidene type, J. Med. Chem. 54 (2011) 8646–8657.
[39] A. Meyer, C.P. Bagowski, M. Kokoschka, M. Stefanopoulou, H. Alborzinia, S. Can, D.H. Vlecken, W.S. Sheldrick, S. Wolfl, I. Ott, On the biological properties of alkynyl phosphine gold(I) complexes, Angew. Chem. Int. Ed. Engl. 51 (2012) 8895–8899.
[40] C. Wetzel, P.C. Kunz, M.U. Kassack, A. Hamacher, P. Bohler, W. Watjen, I. Ott, R. Rubbiani, B. Spingler, Gold(I) complexes of water-soluble diphos-type ligands: synthesis, anticancer activity, apoptosis and thioredoxin reductase inhibition, Dalton Trans. 40 (2011) 9212–9220.
[41] E. Viry, E. Battaglia, V. Deborde, T. Muller, R. Reau, E. Davioud-Charvet, D. Bagrel, A sugar-modified phosphole gold complex with antiproliferative properties acting as a thioredoxin reductase inhibitor in MCF-7 cells, ChemMedChem 3 (2008) 1667–1670.
[42] S. Karcher, H.H. Steiner, R. Ahmadi, S. Zoubaa, G. Vasvari, H. Bauer, A. Unterberg, C. Herold-Mende, Different angiogenic phenotypes in primary and secondary glioblastomas, Int. J. Cancer 118 (2006) 2182–2189.
[43] K. Becker, C. Herold-Mende, J.J. Park, G. Lowe, R.H. Schirmer, Human thioredoxin reductase is efficiently inhibited by (2,2′:6′,2″ -terpyridine)platinum(II) complexes. Possible implications for a novel antitumor strategy, J. Med. Chem. 44 (2001) 2784–2792.
[44] R. Ahmadi, S. Urig, M. Hartmann, B.M. Helmke, S. Koncarevic, B. Allenberger, C. Kienhoefer, M. Neher, H.H. Steiner, A. Unterberg, C. Herold-Mende, K. Becker, Antiglioma activity of 2,2′:6′,2″-terpyridineplatinum(II) complexes in a rat model—effects on cellular redox metabolism, Free Radic. Biol. Med. 40 (2006) 763–778.
[45] I. Ott, H. Scheffler, R. Gust, Development of a method for the quantification of the molar gold concentration in tumour cells exposed to gold-containing drugs, ChemMedChem 2 (2007) 702–707.
[46] S.M. Kanzok, S. Rahlfs, K. Becker, R.H. Schirmer, Thioredoxin, thioredoxin reductase, and thioredoxin peroxidase of malaria parasite *Plasmodium falciparum*, Methods Enzymol. 347 (2002) 370–381.
[47] A. Nordhoff, U.S. Bucheler, D. Werner, R.H. Schirmer, Folding of the four domains and dimerization are impaired by the Gly446–>Glu exchange in human glutathione reductase. Implications for the design of antiparasitic drugs, Biochemistry 32 (1993) 4060–4066.
[48] S. Gromer, L.D. Arscott, C.H. Williams Jr., R.H. Schirmer, K. Becker, Human placenta thioredoxin reductase. Isolation of the selenoenzyme, steady state kinetics, and inhibition by therapeutic gold compounds, J. Biol. Chem. 273 (1998) 20096–20101.
[49] S. Urig, J. Lieske, K. Fritz-Wolf, A. Irmler, K. Becker, Truncated mutants of human thioredoxin reductase 1 do not exhibit glutathione reductase activity, FEBS Lett. 580 (2006) 3595–3600.
[50] S.T. Crooke, C.K. Mirabelli, Molecular mechanisms of action of auranofin and other gold complexes as related to their biologic activities, Am. J. Med. 75 (1983) 109–113.
[51] C.K. Mirabelli, C.M. Sung, J.P. Zimmerman, D.T. Hill, S. Mong, S.T. Crooke, Interactions of gold coordination complexes with DNA, Biochem. Pharmacol. 35 (1986) 1427–1433.
[52] C.R. Wilson, A.M. Fagenson, W. Ruangpradit, M.T. Muller, O.Q. Munro, Gold(III) complexes of pyridyl- and isoquinolylamido ligands: structural, spectroscopic, and biological studies of a new class of dual topoisomerase I and II inhibitors, Inorg. Chem. 52 (2013) 7889–7906.
[53] J.J. Yan, A.L. Chow, C.H. Leung, R.W. Sun, D.L. Ma, C.M. Che, Cyclometalated gold(III) complexes with N-heterocyclic carbene ligands as topoisomerase I poisons, Chem. Commun. (Camb.) 46 (2010) 3893–3895.
[54] O. Rackham, S.J. Nichols, P.J. Leedman, S.J. Berners-Price, A. Filipovska, A gold(I) phosphine complex selectively induces apoptosis in breast cancer cells: implications for anticancer therapeutics targeted to mitochondria, Biochem. Pharmacol. 74 (2007) 992–1002.
[55] S. Prast-Nielsen, M. Cebula, I. Pader, E.S. Arner, Noble metal targeting of thioredoxin reductase–covalent complexes with thioredoxin and thioredoxin-related protein of 14 kDa triggered by cisplatin, Free Radic. Biol. Med. 49 (2010) 1765–1778.
[56] H. Kudo, T. Mio, T. Kokunai, N. Tamaki, K. Sumino, S. Matsumoto, Quantitative analysis of glutathione in human brain tumors, J. Neurosurg. 72 (1990) 610–615.
[57] R.C. Strange, A.A. Fryer, B. Matharoo, L. Zhao, J. Broome, D.A. Campbell, P. Jones, I.C. Pastor, R.V. Singh, The human glutathione S-transferases: comparison of isoenzyme expression in normal and astrocytoma brain, Biochim. Biophys. Acta 1139 (1992) 222–228.
[58] A. Korshunov, A. Golanov, R. Sycheva, I. Pronin, Prognostic value of tumour associated antigen immunoreactivity and apoptosis in cerebral glioblastomas: an analysis of 168 cases, J. Clin. Pathol. 52 (1999) 574–580.
[59] T. Tamura, T.C. Stadtman, A new selenoprotein from human lung adenocarcinoma cells: purification, properties, and thioredoxin reductase activity, Proc. Natl. Acad. Sci. U. S. A. 93 (1996) 1006–1011.
[60] M. Berggren, A. Gallegos, J.R. Gasdaska, P.Y. Gasdaska, J. Warneke, G. Powis, Thioredoxin and thioredoxin reductase gene expression in human tumors and cell lines, and the effects of serum stimulation and hypoxia, Anticancer Res. 16 (1996) 3459–3466.
[61] D.T. Lincoln, F. Al-Yatama, F.M. Mohammed, A.G. Al-Banaw, M. Al-Bader, M. Burge, F. Sinowatz, P.K. Singal, Thioredoxin and thioredoxin reductase expression in thyroid cancer depends on tumour aggressiveness, Anticancer Res. 30 (2010) 767–775.
[62] R. Kemerdere, T. Kacira, H. Hanimoglu, M. Kucur, T. Tanriverdi, B. Canbaz, Tissue and plasma thioredoxin reductase expressions in patients with glioblastoma multiforme, J. Neurol. Surg. A 74 (2013) 234–238.
[63] I.C. Shaw, Gold-based therapeutic agents, Chem. Rev. 99 (1999) 2589–2600.

Please cite this article as: E. Jortzik, et al., Antiglioma activity of GoPI-sugar, a novel gold(I)–phosphole inhibitor: Chemical synthesis, mechanistic studies, and effectiveness *in vivo*, Biochim. Biophys. Acta (2014), http://dx.doi.org/10.1016/j.bbapap.2014.01.006